Detecting nanoscale vibrations as signature of life

Sandor Kasas[a,b], Francesco Simone Ruggeri[a], Carine Benadiba[a], Caroline Maillard[a], Petar Stupar[a], Hélène Tournu[c], Giovanni Dietler[a], and Giovanni Longo[a,1]

[a]Laboratoire de Physique de la Matière Vivante, Institut de Physique des Systèmes Biologiques, Facultè des Sciences des Base, École Polytechnique Fédérale de Lausanne, 1015 Lausanne, Switzerland; [b]Département des Neurosciences Fondamentales, Faculté de Biologie et de Médecine, Université de Lausanne, 1005 Lausanne, Switzerland; and [c]Department of Molecular Microbiology, Vlaams Instituut voor Biotechnologie (VIB), B-3001 Leuven, Belgium

Edited by Robert H. Austin, Princeton University, Princeton, NJ, and approved December 2, 2014 (received for review August 9, 2014)

The existence of life in extreme conditions, in particular in extraterrestrial environments, is certainly one of the most intriguing scientific questions of our time. In this report, we demonstrate the use of an innovative nanoscale motion sensor in life-searching experiments in Earth-bound and interplanetary missions. This technique exploits the sensitivity of nanomechanical oscillators to transduce the small fluctuations that characterize living systems. The intensity of such movements is an indication of the viability of living specimens and conveys information related to their metabolic activity. Here, we show that the nanomotion detector can assess the viability of a vast range of biological specimens and that it could be the perfect complement to conventional chemical life-detection assays. Indeed, by combining chemical and dynamical measurements, we could achieve an unprecedented depth in the characterization of life in extreme and extraterrestrial environments.

nanomechanical sensors | extraterrestrial life | nanoscale fluctuations | living specimens | nanomotion detector

The existence of life in extreme conditions, in particular in extraterrestrial environments, is certainly one of the most intriguing scientific questions of our time. Indeed, the work of many scientists and organizations is focused on the discovery and on the consequent study of extremophiles and extraterrestrial organisms. The direct research for these kinds of life forms is usually conducted by deploying robotic crafts. These man-made vessels contain a suite of scientific analytical instrumentation that is specifically conceived to trace life signatures contained in the geological record. For instance, the search for life in our solar system started in 1975 with the Viking program and continues today. Future missions are planned to explore the presence of life on satellites of the giant planets, such as Europa (Jupiter) or Titan and Enceladus (Saturn). The biological instrumentation that is included in these vessels is complex, but up to now, it is mainly devoted to the chemical detection of molecules involved in living metabolism, as we know it on Earth.

In this report, we show how a technique, the nanomotion detector, can be used in new life-searching instrumentation in Earth-bound and interplanetary missions. The technique exploits the sensitivity of nanomechanical sensors to transduce the small movements that characterize living systems. The intensity of such movements is an indication of the viability of the specimens and conveys information related to their metabolic activity. Here, we demonstrate that this simple technique can assess the viability of a vast range of biological specimens and that it could be the perfect complement to conventional chemical assays. Moreover, due to the simplicity of its working principle, a device based on this technology has negligible weight and requires very low electrical power, compared with other life-detector systems.

Nanomechanical oscillators are extremely sensitive devices that are commonly used to measure very small deflections and detect forces in the order of the piconewton. These sensors can be used to characterize living specimens and their metabolic cycles (1–4). For instance, recent studies have shown how cantilevers can investigate the activity of a cell's molecular motors (5), enzymes adsorbed on mica (6), or the particular vibrations of living *Saccharomyces cerevisiae* (7, 8). Overall, these extremely powerful and versatile sensors are capable of characterizing biological systems with unprecedented detail and time resolution and are nowadays used for several biological applications (9–16).

To extend the scope of the scientific problems that can be investigated with this tool, we have recently demonstrated how nanomechanical oscillators can be used to study nanometer-scale movements in biological specimens (17). In this pioneering work, we have exploited this nanomotion detector to monitor the viability of bacteria in the presence of different antibiotics and to assess rapidly (in less than 30 min) a complete bacterial antibiogram (18). Recently, other groups have used our technique to confirm our findings and to study the fluctuations induced by bacteria on a cantilever (19).

The working principle of the technique may be summarized as follows. A microfabricated atomic force microscopy (AFM) cantilever is inserted into an analysis chamber, and specimens are attached to its surface. The cantilever transduces the movements of the samples with a subnanometer resolution. The dynamic deflections of this sensor are detected and recorded using a laser-based transduction system. The time resolution and sensitivity of this system make it ideal to study living specimens at the nanoscale. It can be operated in air or in a liquid environment; in this latter case, the living specimens can be exposed to triggering or inhibiting chemicals to characterize their response to the stimuli (Fig. 1). Furthermore, the small size, relative simplicity, and versatility of the setup open the way to its parallelization: several single detectors can be used at the same time to form a complex laboratory-on-a-chip system capable of detecting and characterizing unknown living organisms.

Here, we demonstrate the use of this sensor to study a large range of biological specimens, ranging from prokaryotic to eukaryotic organisms. The motion and metabolic state of all

Significance

The quest to find life in extreme and extraterrestrial environments is exciting and touches many research fields. One of the common signatures of life is movement: Even small microorganisms vibrate in response to their metabolic activity. Thus, we have devised a nanomotion detector to study these fluctuations and to associate them to the metabolic activity of the specimens. This technique does not measure the chemical response of life, which would require prior knowledge of the metabolic pathways involved. Instead, it monitors the physical manifestation of any kind of metabolic activity the microorganisms might have. Here, we show how this nanomotion detector can study any living system, paving the way to a complementary approach to the study of life in extreme environments.

Author contributions: S.K., G.D., and G.L. designed research; F.S.R., C.B., C.M., P.S., and G.L. performed research; C.B., C.M., and H.T. contributed new reagents/analytic tools; S.K., F.S.R., and G.L. analyzed data; and S.K. and G.L. wrote the paper.

The authors declare no conflict of interest.

This article is a PNAS Direct Submission.

[1]To whom correspondence should be addressed. Email: giovanni.longo@epfl.ch.

This article contains supporting information online at www.pnas.org/lookup/suppl/doi:10.1073/pnas.1415348112/-/DCSupplemental.

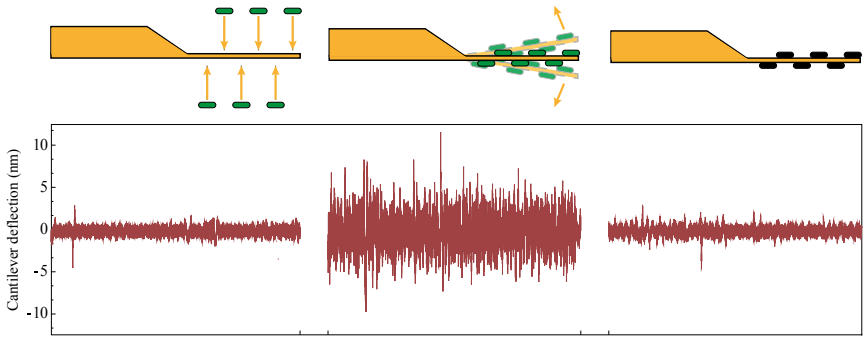

Fig. 1. Detailed depiction of a nanomotion detection experiment. Before the attachment of the living specimens to the sensor, the fluctuations are small (*Left*). When the specimens are immobilized on the sensor, its fluctuations increase (*Center*). Finally, if the microorganisms are killed, through a chemical or physical agent, the sensor reverts to small fluctuations (*Right*).

these systems were artificially activated and repressed by exposing the samples to appropriate chemical components, to demonstrate that the detection system can be used as a simple, extremely sensitive, and weight-efficient "life detector." In each experiment, we immobilized living samples on the cantilever sensor, and we monitored the evolution of its fluctuations over time. We investigated the viability of a wide range of single cellular living organisms. Among bacteria and yeasts, we studied Gram-negative motile *Escherichia coli* (Fig. 2*A*), Gram-positive nonmotile *Staphylococcus aureus* (Fig. 2*B*), and *Candida albicans* yeast cells (Fig. 2*C*). Measurements were also carried out on eukaryotic cells, such as mouse osteoblasts (MC3T3-E1) (Fig. 3*A*), human neuroblasts (M17) (Fig. 3*B*), and plant cells (*Arabidopsis thaliana*) (Fig. 3*C*). A detailed description of the experimental protocols and of the individual experiments is presented in *SI Text*.

In all cases, the presence of the living systems on the cantilever surface produced an increase in the amplitude of the measured fluctuations. The experimental evidence suggests that these fluctuations reflected the metabolic state of the microbes or of the cells. Indeed, upon the injection of nutrients into the analysis chamber, the amplitude of the oscillations increased whereas the exposure to inhibiting agents stopped the movements of the cantilever, indicating that the chemical affected the specimens. To better visualize the macroscopic effects of the stimuli, some experiments were performed while imaging the cantilever with a conventional optical microscope (examples for each experiment are shown in the respective panels in Fig. 2 for microorganisms and Fig. 3 for cells whereas Movies S1–S3 show a time-lapse reconstruction of the microscopic movements of the eukaryotes throughout an entire experiment). Comparing the optical images with the nanomotion data gives insight into the

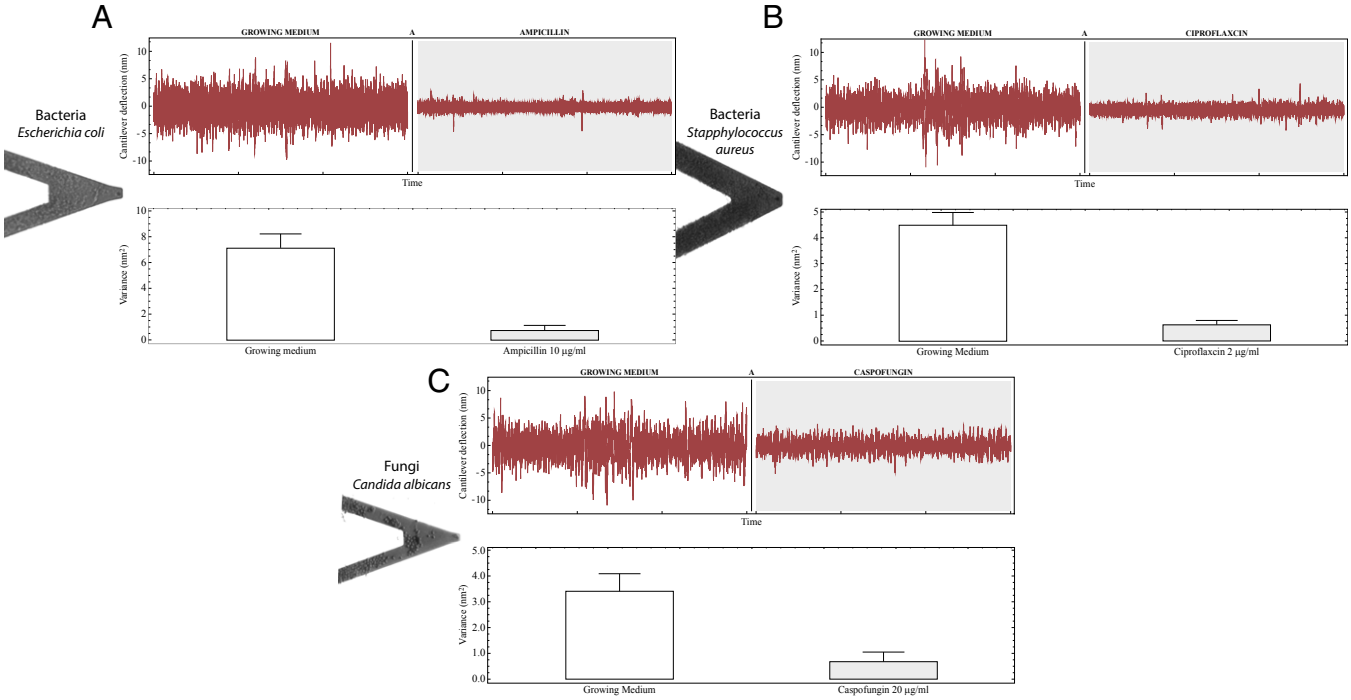

Fig. 2. Experiments on bacteria and yeasts. (*A*) Experiment involving *E. coli*. Two typical 10-min segments of the sensor's fluctuations are shown: the living bacteria induced a large fluctuation of the sensor whereas, 15 min after injection of a bactericidal dose of ampicillin, the fluctuations were largely reduced. (*B*) Experiment involving *S. aureus* exposed to a bactericidal dose of ciproflaxcin. Here, we present two typical 10-min segments of the fluctuations in buffer and after exposure to the antibiotic. (*C*) Experiment involving *C. albicans* exposed to a fungicidal dose of caspofungin. We show typical 2-min segments of the sensor's fluctuations before and after exposure to the antifungal.

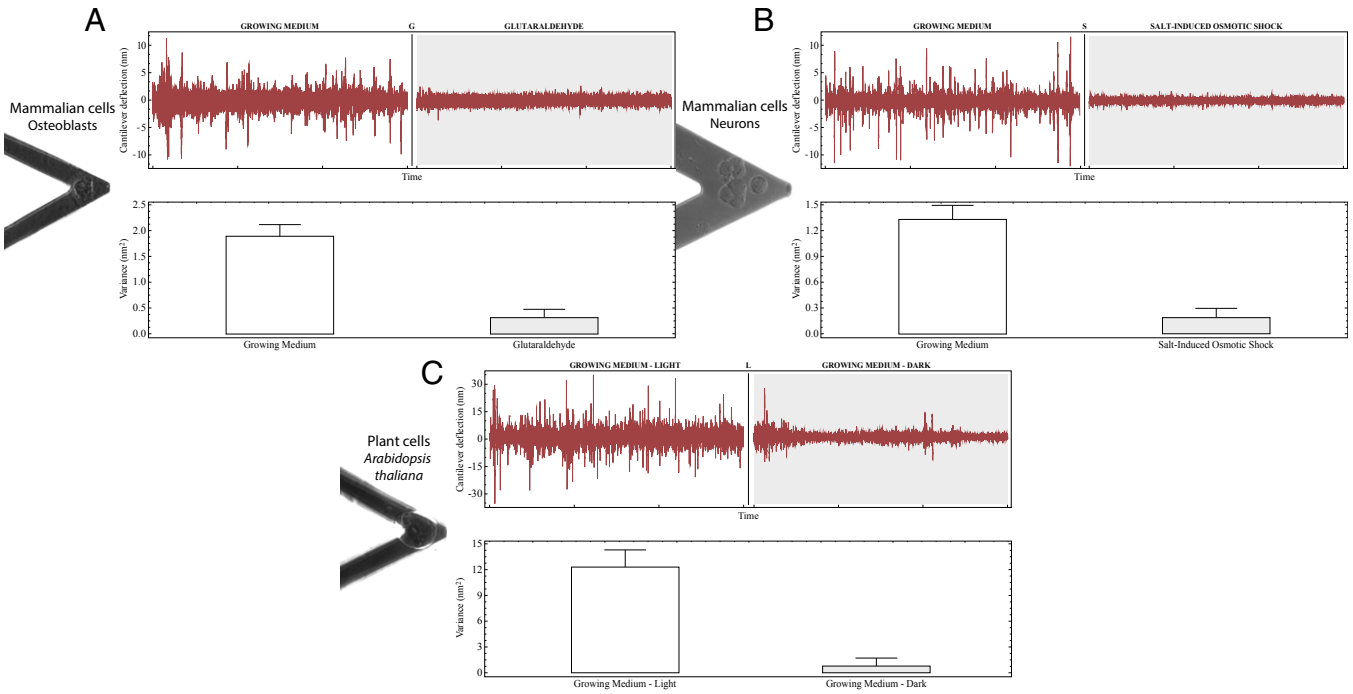

Fig. 3. Experiments on eukaryotic cells. (*A*) Experiment on osteoblast cells. Two typical 10-min segments of the sensor's fluctuations are shown: a cell was attached to the sensor, and its movements induced large fluctuations. When the cell was killed through chemical fixation, the fluctuations were reduced. (*B*) Experiment involving neuroblast cells. Here, we present two typical 10-min segments of the fluctuations in buffer and after inducing the death of the cells through osmotic shock. (*C*) Experiment involving *A. thaliana* cells. We show typical 2-min segments of the sensor's fluctuations while keeping the cell illuminated and after a prolonged period in a dark environment, which induced the death of the cell. We monitored all three experiments using optical images, as shown in Movies S1–S3.

origin of some fluctuation structures. Moreover, the optical images confirmed that the injection of different media, as well as chemical or physical stimuli, did not cause detachment or macroscopic displacement of the cells over the cantilever.

Our previous results show that the fluctuations convey information on the overall metabolism of the specimens and that they are much more than a mere viability test (18, 20). Thus, we performed some experiments specifically designed to understand the origin of the measured fluctuations. We have focused on the pathways involved in the internal motion or in the propulsion of the different specimens and studied the variations of the fluctuations upon their chemical deactivation. In one set of experiments, we studied the effect of the movement of *E. coli*'s flagellum on the overall fluctuation of the sensor. We performed this experiment by exposing the bacteria to a high concentration of glucose solution, which inhibits the motion and, in some cases, even the synthesis of the flagellum (21). These experiments are described in detail in *SI Text* and show that the exposure to glucose caused, at first, an increase in the overall fluctuations, probably induced by the digestion of the added energy source. This first increase was followed by a reduction of the sensor's amplitude, which could be the fingerprint of the inhibition of the flagellum (Figs. S1 and S2).

In other experiments, we investigated the role on the resulting fluctuations of different cytoskeleton components of mammalian cells. Osteoblasts were treated with chemical agents that induced the depolymerization of either the actin (Fig. S3 and Movie S4) or the tubulin cytoskeletal networks (Fig. S4 and Movie S5).

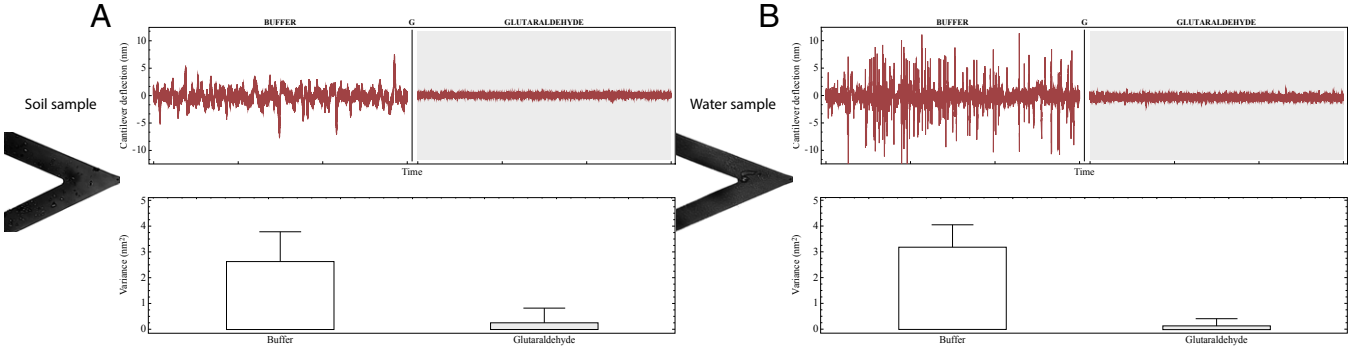

Fig. 4. Experiments involving soil and water samples. (*A*) Typical 4-min segments of the sensor's fluctuations induced by the presence of microorganisms from the soil sample are shown. The viability of the specimens caused large fluctuations, and, when glutaraldehyde was introduced to kill all microorganisms, the fluctuations returned to low levels. (*B*) The living systems present in the water samples induced an increase in the amplitude of the movements of the sensor. After chemical fixation, the movements were reduced.

These experiments, recounted in *SI Text*, show that the high temporal resolution of the nanomotion detector evidences two different subgroups of fluctuations, which could represent the signature of the movements of the actin and of the tubulin networks. Specifically, large fluctuations of the sensor can be associated with movements inside the actin network whereas less intense but more frequent fluctuations can be attributed to the tubulin network. Naturally, some more studies will be needed to understand fully all of the components of the signal produced by living systems. In fact, we have recently demonstrated that even small conformational changes in proteins can induce fluctuations of the cantilever sensor (22). Thus, we can conclude that nanoscale movement is a universal signature of life and that every living system exhibits a large and diverse variety of movements that are related directly to their viability.

One remarkable peculiarity of the nanomotion detector is that it does not need a complete characterization of the specimens under investigation to detect their presence and viability. In fact, we were able to perform completely blind experiments in which the samples were originated from uncontrolled sources and completely unknown. We collected some dry soil from the fields and some water from the river Sorge, near our university campus. A first simple optical microscopy investigation evidenced the presence of different kinds of microorganisms, including bacteria and small unicellular species. We performed a nanomotion detection investigation: just like in the other controlled experiments, we diluted the samples in the analysis chamber and immobilized them on the cantilevers. Next, we measured the fluctuations of the sensors in a buffer solution. The fluctuations of the cantilever are shown in Fig. 4 and confirm that the soil (Fig. 4*A*) and water samples (Fig. 4*B*) contain living specimens. Their movements on the sensor's surface caused large fluctuations of the cantilever whereas, by chemically inducing their death, these fluctuations were greatly reduced.

Remarkably, in each of the experiments described in this work, we needed just a few tens of minutes to determine the presence of viable microorganisms. Moreover, a very small number of living specimens diluted in just a few microliters of solution were sufficient to perform the experiments.

These results demonstrate that this technique can efficiently identify the activity produced by a wide range of living organisms that inhabit Earth and that, in some cases, the collected data can help identifying the specific signature of particular cellular movements. Even if the sample under investigation is not characterized, the nanomotion detector can rapidly and reliably deliver information on its viability. In fact, whereas most of the conventional life detectors currently used in biology and astrobiology look for the chemical signatures of life, this technique is focused on monitoring a physical quantity: the nanometer-scale movement. This technique offers a complementary point of view in the search for life in extreme habitats. For instance, it could allow the detection of systems with novel and unexpected metabolic pathways. Indeed, by combining chemical and dynamical measurements, we could achieve an unprecedented depth in the characterization of life in extreme and extraterrestrial environments.

Furthermore, these results will be useful to define the physical and chemical limits for life on Earth and to understand the underlying biophysical characteristics of life that set these limits (23). Finally, the simplicity of its working principle and the possibility to miniaturize and parallelize the apparatus make this device a good candidate to be embarked in future life-seeking spaceships.

Methods

To perform the experiments, we used commercial silicon nitride, microfabricated 200-μm-long cantilevers, with a nominal spring constant of 0.06 N/m (DNP-10 Bruker). The oscillations of this lever were detected through the deflection of the laser beam of a commercial AFM; for all of the presented experiments, we used a Nanowizard III (JPK). The data analysis was completed with custom software written in LabView (National Instruments).

The typical setup of the experiments is described in detail in our previous works (18, 20). Briefly, a typical experiment started by depositing the specimen of interest onto the sensor, which was preliminarily functionalized with a linker molecule. Depending on the particular system under investigation, we chose the functionalization that had demonstrated the best immobilization efficiency. For bacteria, yeast, and plant cells, we chose glutaraldehyde; for neuron cells, we functionalized the sensor with poly-L-lysine; and osteoblasts required a fibronectin coating (see the *SI Text* for a detailed description of the cantilever preparation for each experiment). The fluctuations of the cantilever were recorded in nourishing media and were used to define the viability of the living organisms. Subsequently, the cantilever was exposed to chemical or physical conditions that brought the living specimens to death, resulting in reduced fluctuations of the sensor. To evaluate the experimental results, the fluctuations of the cantilever were statistically analyzed by calculating their variance.

ACKNOWLEDGMENTS. We thank K. Radotic for helpful discussions regarding *A. thaliana*. We thank Prof. Lashuel's group for providing the neuroblast cells and for helpful discussions. We thank L. Alonso and S. Aghaee for support in the preparation of the experiments. S.K. acknowledges the support of Swiss National Grant 200021-144321. G.L. acknowledges the support of Italian Health Ministry Grant GR-2009-1605007.

1. Boisen A, Dohn S, Keller SS, Schmid S, Tenje M (2011) Cantilever-like micromechanical sensors. *Rep Prog Phys* 74(3):036101.
2. Waggoner PS, Craighead HG (2007) Micro- and nanomechanical sensors for environmental, chemical, and biological detection. *Lab Chip* 7(10):1238–1255.
3. Alvarez M, Lechuga LM (2010) Microcantilever-based platforms as biosensing tools. *Analyst (Lond)* 135(5):827–836.
4. Hansen KM, Thundat T (2005) Microcantilever biosensors. *Methods* 37(1):57–64.
5. Schneider SW, et al. (1999) Continuous detection of extracellular ATP on living cells by using atomic force microscopy. *Proc Natl Acad Sci USA* 96(21):12180–12185.
6. Radmacher M, Fritz M, Hansma HG, Hansma PK (1994) Direct observation of enzyme activity with the atomic force microscope. *Science* 265(5178):1577–1579.
7. Pelling AE, Sehati S, Gralla EB, Valentine JS, Gimzewski JK (2004) Local nanomechanical motion of the cell wall of Saccharomyces cerevisiae. *Science* 305(5687):1147–1150.
8. Pelling AE, Sehati S, Gralla EB, Gimzewski JK (2005) Time dependence of the frequency and amplitude of the local nanomechanical motion of yeast. *Nanomedicine* 1(2):178–183.
9. Ilic B, et al. (2000) Mechanical resonant immunospecific biological detector. *Appl Phys Lett* 77(3):450–452.
10. Braun T, et al. (2009) Quantitative time-resolved measurement of membrane protein-ligand interactions using microcantilever array sensors. *Nat Nanotechnol* 4(3):179–185.
11. Fritz J, et al. (2000) Translating biomolecular recognition into nanomechanics. *Science* 288(5464):316–318.
12. Godin M, et al. (2010) Cantilever-based sensing: the origin of surface stress and optimization strategies. *Nanotechnology* 21(7):75501.
13. Ndieyira JW, et al. (2008) Nanomechanical detection of antibiotic-mucopeptide binding in a model for superbug drug resistance. *Nat Nanotechnol* 3(11):691–696.
14. Lang HP, et al. (1999) An artificial nose based on a micromechanical cantilever array. *Anal Chim Acta* 393(1-3):59–65.
15. McKendry R, et al. (2002) Multiple label-free biodetection and quantitative DNA-binding assays on a nanomechanical cantilever array. *Proc Natl Acad Sci USA* 99(15):9783–9788.
16. Djuric ZG, Jokic IM (2007) Thermomechanical noise of nanooscillators with time-dependent mass. *Microelectron Eng* 84(5-8):1639–1642.
17. Kasas S, Longo G, Alonso-Sarduy L, Dietler G (2011) Swiss patent extended internationally PCT/IB2011054553.
18. Longo G, et al. (2013) Rapid detection of bacterial resistance to antibiotics using AFM cantilevers as nanomechanical sensors. *Nat Nanotechnol* 8(7):522–526.
19. Lissandrello C, et al. (2014) Nanomechanical motion of Escherichia coli adhered to a surface. *Appl Phys Lett* 105(11):113701.
20. Aghayee S, et al. (2013) Combination of fluorescence microscopy and nanomotion detection to characterize bacteria. *J Mol Recognit* 26(11):590–595.
21. Adler J, Templeton B (1967) The effect of environmental conditions on the motility of Escherichia coli. *J Gen Microbiol* 46(2):175–184.
22. Alonso-Sarduy L, et al. (2014) Real-time monitoring of protein conformational changes using a nano-mechanical sensor. *PLoS ONE* 9(7):e103674.
23. Trent JD (2000) Extremophiles in astrobiology: Per ardua ad astra. *Gravit Space Biol Bull* 13(2):5–11.

Supporting Information

Kasas et al. 10.1073/pnas.1415348112

SI Methods

Substrates, Enzymes, and Reagents. All chemicals, PBS (pH 7.4), lysogeny broth (LB), standard yeast medium (RPMI-1640 R6504), (3-aminopropyl)triethoxysilane (APTES), poly-L-lysine, Trypsin-EDTA, cytochalasin, 2,4-dichlorophenoxybutyric acid, fibronectin, glucose, glutaraldehyde, cytochalasin, nocodazole, ciproflaxcin, and ampicillin, all with analytical grade, were supplied by Sigma-Aldrich. The culture mediums for mammalian cells were supplied by Life Technologies. The α-MEM medium was provided by GIBCO-Life Technologies. The medium for the culture of the plant cells was acquired from Duchefa Biochemie.

Preparation of *Escherichia coli* for Viability Nanomotion Analysis. Frozen stocks of *E. coli* DH5α-strain were stored at −80 °C in glycerol-supplemented LB. In preparation for the experiments, these bacteria were streaked on agar media. A few bacterial colonies were then collected and incubated overnight at 37 °C in 1 mL of LB. After incubation, the bacteria were washed three times in PBS. Between each rinse, they were sedimented by centrifugation at 2,300 × *g* for 10 min and were finally resuspended in 0.5 mL of PBS. This concentrated solution was used in the nanomotion experiments.

Preparation of *E. coli* for Flagellum Inhibition and Swarming Tests. Frozen stocks of *E. coli*, C-strain, were stored at −80 °C in glycerol-supplemented LB. In preparation for the experiments, these bacteria were streaked on agar media. A few bacterial colonies were then collected and incubated overnight at 37 °C in 1 mL of LB. After this first incubation, 20 μL of bacteria-rich solution was inoculated into another, fresh growth media and left to grow for 5 h to midexponential phase. When this second incubation reached an optical density (OD_{595}) of 0.7, the bacteria were washed three times in PBS. Between each rinse, they were sedimented by centrifugation at 1,400 × *g* for 5 min and were finally resuspended in 0.5 mL of PBS. This final concentrated solution was immediately used in the flagellum inhibition experiments and for the swarming tests.

Preparation of *Staphylococcus aureus*. As in the case of *E. coli*, a few colonies of *S. aureus*, Newman strain, were collected from an agar plate and incubated overnight at 37 °C in 1 mL of LB. After incubation, the bacteria were washed three times in PBS and finally resuspended in 0.5 mL of PBS, as described above. This concentrated solution was used in the nanomotion experiments.

Preparation of *Candida albicans*. *C. albicans* cells have the ability of adapting to their environment and to grow either in yeast (ovoid) or hyphae (filamentous) forms. We cultivated the WT (SC5314) cells to drive them to their yeast form: they were incubated at 27 °C overnight in 15 mL of standard yeast medium. After incubation, the *C. albicans* cells were washed three times in PBS. Between each rinse, they were sedimented by centrifugation at 1,000 × *g* for 10 min and were finally resuspended in 0.5 mL of PBS. This concentrated solution was used in the nanomotion experiments.

Preparation of Osteoblast Cells. Murine osteoblast-like MC3T3-E1 cells (from European Collection of Cell Cultures) were cultured in humidified air under 5% CO_2 at 37 °C in α-MEM medium with 10% (vol/vol) FBS and 2 mM L-glutamine (osteoblast medium). Osteoblast cells were detached from the culture flask with Trypsin-EDTA treatment of 5 min at 37 °C, before being used in the nanomotion experiments.

Preparation of Neuroblast Cells. The M17 neuroblast cells are commercially available from the ATCC, and, for our experiments, we used the cells kindly provided by the Laboratory of Molecular and Chemical Biology of Neurodegeneration-École Polytechnique Fédérale de Lausanne (EPFL) group supervised by H. A. Lashuel (EPFL, Lausanne, Switzerland). The cells were cultured in humidified air under 5% CO_2 at 37 °C in a mix of F12 medium and DMEM, supplemented by 10% (vol/vol) FBS (neuroblast medium). The neuroblast cells were detached from the culture flask with Trypsin-EDTA treatment of 5 min at 37 °C, before using them in the nanomotion experiments.

Preparation of *Arabidopsis thaliana*. *A. thaliana* suspension cells were kindly provided by the Hartdke laboratory at the Department of Plant Molecular Biology (Lausanne University, Lausanne, Switzerland) and were cultured at 21 °C under continuous 130 μE light while shaking at 120 rpm. Cells were subcultured every 14 d by adding 3 mL of the cell suspension to a 100-mL flask containing 30 mL of Gamborg B5 medium (1), autoclaved, pH adjusted to 5.7, and reconstituted from Gamborg Vitamin mixture 1,000× and supplemented by addition of 2,4-dichlorophenoxybutyric acid. The cells were then diluted 100 times in Gamborg medium and prepared for the nanomotion experiments.

Preparation of Soil Samples. A few milligrams of dry soil were collected from the fields surrounding the EPFL Cubotron building in Lausanne. The soil was immediately diluted in 5 mL of PBS and agitated for 5 min and, finally, left at 37 °C for 1 h. After this period, the heavier particles had deposited, and we were able to collect 2 mL of the supernatant. At this point, we followed the same protocol we used in the case of the preparation of the bacterial samples: we sedimented the samples twice by centrifugation at 2,300 × *g* for 10 min and resuspended the pellet in 0.5 mL of PBS. This concentrated solution was used in the nanomotion experiments.

Preparation of Water Samples. One hundred milliliters of water were collected from the Sorge river, flowing close to the EPFL Cubotron building in Lausanne. We immediately sedimented the water samples by centrifugation at 2,300 × *g* for 10 min and diluted the resulting pellet in 0.5 mL of PBS. This concentrated solution was used in the nanomotion experiments.

SI Description of the Setup

To perform the measurements, we used a JPK Nanowizard III AFM (JPK) coupled with an Axiovert X optical microscope (Zeiss Microscopy). All of the optical images were collected using a standard 40× objective through a Progres MFCool digital camera (Jenoptik). The in-program camera control software was used to collect the images in an automated way. The AFM was equipped with a custom liquid cell (2) to reduce the amount of liquid medium needed to perform the measurements and to allow a noiseless medium transition during the experiments.

Injection System. Different imaging buffers were assayed using a gravity injection system based on the one published by Thomson et al. (3). To ensure a complete exchange of the fluid, 400 μL of each solution were injected at a flow rate of 0.1–8 μL/s. This injection system allowed exchanging the fluid several times in

a single experiment, and thus the chemical environment in which the deflection measurement was being conducted.

Temperature Control. The temperature control is a crucial parameter when performing experiments using cantilevers as nanomechanical sensors. We controlled this parameter by placing the microscope in a temperature-controlled room, and all of the solutions were left to thermalize for minimally 1 h before starting the experiments. The temperature of all of the injected media was controlled just before the injection using a bimetallic temperature sensor (DT120; Rüeger). This in-depth control ensured that the temperature throughout the entire experimental analysis was constant within 0.1 °C. Before starting any acquisition, we waited for the system to stabilize; less than 30 min were needed to obtain a perfectly stable cantilever.

Sensor Preparation and Characterization. In all our experiments, we used silicon nitride triangular cantilevers (DNP-10; Bruker) with a nominal length of 205 μm and spring constant of 0.06 N/m.

For the experiments involving bacteria and yeasts, as well as in those regarding the uncontrolled soil and water samples, we functionalized the cantilever with glutaraldehyde (0.5% for 7 min) followed by thorough rinsing with ultrapure water (4, 5). We dried the treated sensor using nitrogen, exposed it to a small volume (30 μL) of the solution containing the live specimens, and, finally, left it to incubate at room temperature for 30 min. After such incubation, the cantilever was inserted into the tip-holder and immediately introduced into the analysis chamber, which was flushed with PBS.

In a similar way, to deposit neuron cells on the cantilever, we functionalized the sensor with poly-L-lysine (10% for 30 min) and we rinsed it thoroughly using ultrapure water. Then, we deposited on the sensor a small droplet (~10 μL) of the solution containing the live cells, and we left it to incubate at 37 °C for 2 h in DMEM media. This first incubation was useful for neurons deposition on the lever. At the end of this period, the sensor was ready for the nanomotion experiments.

The experiments involving the osteoblast cells were performed using cantilevers functionalized with fibronectin (10 μg/mL for 15 min). The sensor was then inserted into the analysis chamber, which was flushed with a cellular nourishing buffer containing a small concentration of live cells. At this point, we used the AFM coarse and fine movement capabilities to "fish" a single cell (6), attaching it near the apical region of the cantilever.

Finally, for the experiments involving the plant cells, we used glutaraldehyde-coated cantilevers (5% for 10 min), which were washed thoroughly upon insertion in the analysis chamber. Then, as in the case of the osteoblast cells, we used the movement of the AFM to fish a cell and attach it to the sensor.

Calibration of the Cantilever. Each cantilever was characterized in the fluid environment using the thermal fluctuation method (7, 8) to calculate its resonance frequency and the effective spring constant (which were in good agreement with the nominal values). By performing a force curve on a clean hard surface, we were able to determine the sensitivity of the transduction system and to convert the output voltage into effective deflections on the nanometer scale. Such preliminary characterizations were performed on each cantilever and several times during each experiment to fully characterize the sensor and control the eventual variations induced by the presence of the bacteria.

Measurement of the Nanomotion of the Specimens. The time-dependent fluctuations of the sensor were recorded through a dedicated electronic system. The cantilever deflection data were collected using a data acquisition board (BNC-2110; National Instruments) and LabVIEW software (National Instruments). Because the typical timescale of bacteria and cells is between some seconds and some milliseconds (9), the cantilever fluctuations were recorded with an adequate temporal resolution (a sampling frequency of 10 kHz was chosen).

The stability of the liquid in the analysis chamber was crucial in our experimental setup. So, after injecting each medium, we waited at least 5 min to ensure that the liquid had stabilized before starting the measurement. The injection of new media in the analysis chamber was performed at very slow rates, always verifying through the optical images that the samples on the cantilever sensor were unaffected by the flow. After the injection and the stabilization period, we activated the fluctuation measurement for minimally 30 min. After this time period, the next solution (for example, one containing glutaraldehyde or a bactericidal dose of antibiotic) was injected into the system.

The exact way in which the cantilever sensors are capable of transducing the movements of the living organisms in measurable fluctuations is still an open question. All of the experimental evidence is quite definitive in indicating that the movements are related to the metabolic activity of the specimens under investigation. In the case of mobile samples, such as *E. coli* or mammalian cells, the movements are probably linked to the motion of pili or flagella or to various cytoskeleton rearrangements. On the other hand, for immobile samples, the issue is more complex, and we suspect that a component of the oscillations of the cantilever could be induced by conformational changes of molecules or ionic channels located on the membrane of the microorganisms.

Deflection Data Analysis. The raw, unfiltered data were analyzed using LabView software developed to analyze the deflection signal, to divide it into 20-s chunks, and to calculate the variance of each chunk. The deflection as a function of time and the corresponding variance function were used to characterize the fluctuations.

SI Detailed Description of Life-Detection Experiments

The Experiments Involving Bacteria: *E. coli*. The cantilever treated with glutaraldehyde and bearing attached the *E. coli* bacteria was inserted into the analysis chamber, which was filled with the bacterial medium (LB). We waited a few minutes to stabilize the liquid in the chamber, and then we monitored the fluctuations of the sensor. The living bacteria induced a large fluctuation of the sensor (a 10-min segment of these fluctuations is shown in Fig. 2*A*, *Left*, average variance ~7.2 nm^2). After 30 min of measurement, we flushed the chamber with a medium containing a bactericidal dose (10 μg/mL) of the antibiotic ampicillin. Next, after 10 min needed to stabilize the chamber, we resumed monitoring the fluctuations, which seemed greatly reduced (Fig. 2*A*, *Right*, average variance of ~0.7 nm^2). At the end of the experiment, the cantilever was extracted from the analysis chamber and incubated in LB at 37 °C overnight to confirm the death of the microorganisms.

The Experiments Involving Bacteria: *S. aureus*. The sensor with the attached *S. aureus* was introduced into the analysis chamber, and the chamber was filled with bacterial growth medium (LB). We waited 10 min to stabilize the system and activated the acquisition system to measure the fluctuations of the sensor as a function of time. The living bacteria present on the cantilever produced the movement of the sensor, as indicated in Fig. 2*B*, *Left* (a typical 10-min segment is shown, average variance ~4.0 nm^2). After ~30 min, we flushed the chamber with a medium containing a bactericidal dose (2 μg/mL) of ciprofloxacin, an antibiotic to which these germs are susceptible. Less than 10 min after the antibiotic injection, the fluctuations were reduced (Fig. 2*B*, *Right*, average variance of ~0.7 nm^2). At the end of the experiment, the cantilever was extracted from the analysis chamber and incubated in LB at 37 °C to confirm the death of the bacteria.

The Experiments Involving Yeasts: *C. albicans*. We introduced the cantilever with the attached *C. albicans* cells into the analysis chamber, which was flushed with the yeast growing medium. After a few minutes of stabilization time, we monitored the movements of the sensor as a function of time. The viability of the *C. albicans* cells was indicated by the amplitude of the fluctuations (average variance ~3.3 nm^2). A 2-min portion of these fluctuations is depicted in Fig. 2*C*, *Left*. After 1 h of measurement, we flushed the chamber with a medium containing a fungicidal dose (20 μg/mL) of the antifungal drug caspofungin. After a second stabilization period of 10 min, we monitored the fluctuations, which were greatly reduced (Fig. 2*C*, *Right*, average variance of ~0.7 nm^2). At the end of the experiment, the cantilever was extracted from the analysis chamber and was incubated in the yeast medium to confirm the death of the microorganisms.

The Experiments Involving Mammalian Cells: Mouse Osteoblasts. A cantilever functionalized for the attachment of osteoblast cells was introduced into the analysis chamber filled with the osteoblast medium, which was kept at 37 °C throughout the entire experiment. A very small concentration of osteoblast cells was injected into the chamber. When these cells had approached the bottom surface of the chamber, we used the coarse and fine movement capabilities of the AFM microscope to bring the cantilever in light contact with one cell. Once we confirmed the cell's attachment to the sensor's surface, we retracted the cantilever 100 μm from the surface, and we started monitoring the movements of the cell. We coupled the analysis of the fluctuations of the sensor (a 10-min section is shown in Fig. 3*A*) with the optical investigation of the cell (Movie S1 shows a sequence of optical images collected every 20 s). The fluctuations of the sensor were stable and high, reflecting the viability of the cells (average variance ~1.8 nm^2). After ~2 h of measurement, we flushed the chamber with a medium enriched with 5% glutaraldehyde, which fixed the cells and brought them rapidly to death. The fluctuations of the sensor consequently reduced in amplitude and stabilized to a very low value (Fig. 3*A*, *Right*, average variance ~0.3 nm^2).

The Experiments Involving Mammalian Cells: Human Neuroblasts. The neuroblast cells were attached to the cantilever, which was then introduced into the analysis chamber filled with the neuroblast medium. Next, we monitored the movements of the sensor as a function of time while recording every 20 s an optical image of the cells on the sensor. The fluctuations of the sensors described the nanometer-scale movements of the cells (a typical 10-min section is shown in Fig. 3*B*, *Left*, average variance ~1.3 nm^2) whereas the optical images depicted their micrometer-sized evolution on the cantilever surface (Movie S2). After ~4 h, we produced an osmotic shock on the cells by increasing the concentration of salt in the analysis chamber. This treatment caused most of the cells to undergo apoptosis, and the death of the cells was reflected in the fluctuations of the sensor, which dropped to ~0.25 nm^2 (Fig. 3*B*, *Right*). The optical images confirmed that all of the cells had died on the sensor.

The Experiments Involving Plant Cells: *A. thaliana*. We introduced into the analysis chamber a cantilever prepared for plant-cell attachment. The chamber was filled with Gamborg medium, and a very small number of *A. thaliana* cells were injected into the chamber. When the cells had deposited on the bottom of the chamber, we used the coarse and fine movement capabilities of the AFM to bring the cantilever in light contact with one cell. Once the cell was attached, we retracted the sensor 500 μm from the surface, and we started monitoring the movements of the cell. We collected the fluctuations of the sensor (2-min sections are depicted in Fig. 3*C*) while performing, every 20 s, an optical image of the cantilever (Movie S3 shows the sequence of these images). The fluctuations of the sensor were very high (average variance ~12.8 nm^2). The viability of the cell was also shown in the optical images by the movement of vesicles inside the *A. thaliana* cell. After ~4 h, we turned off the light illuminating the cell, and we continued monitoring the fluctuations of the sensor. After ~1 h, the fluctuations abruptly reduced their amplitude and stabilized to a very low value (average variance ~0.7 nm^2), indicating that the *A. thaliana* cell had probably died. In Fig. 3*C*, *Right*, we depict the fluctuations of the sensor collected during this abrupt reduction. We confirmed the death of the cell by reactivating the illumination and verifying that there was no visible vesicle movement remaining.

The Experiments Involving the Soil Sample. The cantilever treated with glutaraldehyde and bearing attached the microorganisms present in the soil was inserted into the analysis chamber, which was filled with PBS buffer solution at room temperature. We waited for a few minutes to stabilize the liquid in the chamber, and then we monitored the fluctuations of the sensor. The specimens induced a fluctuation of the sensor (a typical 4-min segment of these fluctuations is shown in Fig. 4*A*, *Left*, average variance ~2.6 nm^2). After 30 min of measurement, we flushed the chamber with a solution containing a 0.5% glutaraldehyde concentration. Next, we waited for another 10 min and resumed monitoring the fluctuations, which seemed greatly reduced (Fig. 4*A*, *Right*, average variance of ~0.5 nm^2). At the end of the experiment, the cantilever was extracted from the analysis chamber and incubated in LB at 37 °C overnight to confirm the death of any microorganism. The entire experiment was recorded using optical images to confirm the continued presence of the microorganisms on the cantilever surface.

The Experiments Involving the Water Sample. The cantilever treated with glutaraldehyde and bearing attached the microorganisms present in the water sample was inserted into the analysis chamber, which was filled with PBS buffer solution at room temperature. We waited for a few minutes to stabilize the liquid in the chamber, and then we monitored the fluctuations of the sensor. The presence of living specimens was confirmed by optical imaging and induced a fluctuation of the sensor (a 20-min segment of these fluctuations is shown in Fig. 4*B*, *Left*, average variance ~3.2 nm^2). After 30 min of measurement, we flushed the chamber with a solution containing a 0.5% glutaraldehyde concentration. Next, we waited for another 10 min, and we resumed monitoring the fluctuations, which seemed greatly reduced, dropping to ~0.25 nm^2 average variance (Fig. 4*B*, *Right*). As for the other experiments, the cantilever was finally extracted from the analysis chamber and incubated in LB at 37 °C overnight to confirm the death of any microorganism. We acquired a time-lapse movie of the entire experiment to confirm the continued presence of the microorganisms on the sensor.

SI Experiments Designed to Investigate the Origin of the Fluctuations

Understanding the origin of the fluctuations is of fundamental importance to describe correctly the biological events that are taking place on the cantilever surface. Furthermore, a more detailed comprehension of the sensor's movements is the key to improving the overall technique and to allowing extracting more information from each experiment. Thus, we performed some control experiments specifically conceived to investigate this issue.

The Movement Contribution of the Flagellum in *E. coli*: Nanomotion Experiments. The interpretation of the fluctuations induced by bacteria on a cantilever surface is a complex task. Such complexity is due, on one side, to the large number of microbes typically attached to the sensor and, on the other, to the diverse interactions that each bacterium has with the surface. The typical overall outcome of the presence of living bacteria on a cantilever

is an almost uniform increase in noise, which has no specific components that can be definitely related to particular metabolic cycles of bacteria. However, we attempted some experiments to obtain a partial interpretation of the measured movements.

Bacterial motility is usually driven by the presence of a gradient in some chemical stimulus and drives the bacterium toward attractants, or away from repellents. Some bacterial species exhibit a particular appendage, called flagellum, which they use to direct and accelerate their movements. This motor system is an extremely complex biological machine and, in the case of *E. coli*, involves the activation and regulation of more than 40 genes (10). Therefore, we focused on this molecular motor to determine its signature on the data we are capable of transducing.

The rate and frequency of the flagellum cycle have already been studied with some detail, showing that these appendages change the rate of their movement as a consequence of a chemical gradient (chemotaxis) (11). Other works have also shown that bacteria, in particular conditions, tend to reduce the motion of their flagella and can even halt their synthesis (12). These peculiar conditions include high salt content, presence of ethanol, or even a high glucose concentration (13, 14).

At first, in our nanomotion experiments, we kept the sensor bearing the bacteria in LB. Next, we added a high concentration of glucose (5 mg/mL) to this medium. The nanomotion detection experiments, shown in Fig. S1, show that the bacteria in LB produced a fluctuation with roughly constant variance, but the average value changed upon injection of the glucose. Minutes after the injection, the overall movement seemed to increase, in good agreement with our previous findings. After this surge, the movement started reducing its range and stabilized at a fluctuation level that was even smaller than the average level measured in the LB. The best interpretation of the evolution of the dynamics of the sensor over time is that the bacteria, once exposed to a large amount of glucose, at first activated their metabolic cycles to digest this abundant energy source. After some time, the constant intake of glucose induced the down-regulation (catabolite repression) of many genes involved in the flagellum movement and production, inducing the microbes to reduce this movement or even discard their flagella, to minimize the, now unnecessary, activity (12).

The Movement Contribution of the Flagellum in *E. coli*: Swarming Tests. The conventional assay to study motility in bacteria is the swarming test. In this test, a small droplet of bacteria is placed in the center of a soft-agar plate and incubated at 33 °C for 40 h. At the end of this period, the size of the colony in the agar is indicative of the flagellar activity in the bacteria. Nonswarming cells are unable to spread across the surface and grow as a confined colony in the center of the plate (15). In our experiments, we compared the size of the colonies formed by bacteria that were exposed to LB broth with 5 mg/mL glucose with the colonies produced by bacteria grown in conventional LB broth. The bacteria grown in glucose exhibit a very small, round colony, with well-defined borders and centered in the spot where the original droplet was placed (Fig. S2). On the other hand, the bacteria grown in LB produce a larger colony, with nondefined form and with smooth borders. In conclusion, the swarming assays confirmed that the bacteria grown in LB exhibit a functioning flagellum whereas the bacteria cultured in LB plus glucose maintain their viability but seem to be much less motile (12).

The Movement Contribution of the Actin Network in Osteoblasts. Compared with the study on bacteria, the experiments on mammalian cells have the advantage of the additional information produced by the time-lapse movies of the cells growing on the surface of the sensor. The analysis of these movies show that, after their first attachment to the cantilever, the cells extend their filopodia and other appendages to spread on the substrate and to ensure a stable adhesion. This first step is followed by large movements in these extended regions of the cell, typically associated with actin network rearrangements, which can be seen with conventional optical microscopy (see, for example, Movie S1). By exposing the cells to a chemical agent that depolymerizes the actin filaments, this particular movement is disrupted, but the overall cell viability is not compromised over time periods of more than 5 h (16). In fact, as shown in Movie S4, after removing the agent, the cells were capable of rebuilding their actin skeleton and of returning to a normal activity, including the visible actin rearrangements (17).

To investigate the effect on the cantilever fluctuations of these actin movements, we monitored osteoblast cells before and after the exposure to cytochalasin, and we followed their evolution after removing the drug. To exploit fully the time resolution of the nanomotion detector and to discriminate the different components of the movements, we divided the fluctuation data in 30-s chunks. We calculated the variance from each of these chunks to follow the evolution of the movements of the cells at this small time scale. As shown in Fig. S3, in buffer, when the cells extend their appendages on the cantilever surface and the actin cycles start, the fluctuation graph evidences large spikes (>10 nm), separated by smaller spikes (>2 nm) and by a lower constant activity (basal fluctuation).

The introduction of the cytochalasin (5 μg/mL) induces large modifications on the morphological point of view, but, once the depolymerization process has completed, only one component of the nanomotion data seemed to be affected. Although the basal fluctuation was still high and the small spikes were still visible, indicating the continued cell viability, the large spikes disappeared. This effect indicates that the large, >10 nm spikes are probably the nanomotion reflection of the movements in the actin network.

Remarkably, the immediate cell's response to the removal of the cytochalasin was an overall reduction of the motion, with a large reduction of all components of the fluctuation that lasted several tens of minutes. We can speculate that this reduction is compatible with a metabolic reorganization of the cell to restart the production of the actin network. After this period, the cells increased their movement, probably in the effort to reconstruct the cytoskeleton. Finally, this reorganization period was followed by a return to a normal activity, described by the reappearance of the large fluctuations spikes.

Additionally, through these experiments, we were able to obtain indications on the possible origin of the low-amplitude basal fluctuations. Indeed, when the actin layer was depolymerized, it did not influence this component, which remained largely unscathed. When we removed the chemical agent responsible for the depolymerization, the cells were able to restore their cytoskeleton integrity. As consequence, we measured an increase of the basal fluctuation level and of the overall variance of the fluctuations.

The Movement Contribution of the Tubulin Network in Osteoblasts. In addition to the external actin network, a deeper network composed of tubulin forms the cellular cytoskeleton. Although this second layer is less responsible for the overall movement of the cell, we can still highlight its cycles and redistributions by means of the nanomotion detector. We performed some experiments on osteoblasts exposed to 0.2 μg/mL nocodazole, a drug that induces the depolymerization of microtubules. As for the case of cytochalasin, the movements of the cells exposed to such a low concentration of this chemical agent reflect the loss of this component of the cytoskeleton, but the overall cell viability is not compromised (18). Remarkably, even in the presence of the nocodazole, the optical images showed clearly structures moving in the cellular membranes, which are similar to the rearrangements of the actin network we have described in the previous paragraph (Movie S5). This observation is consistent with literature

results, which showed that, in the presence of nocodazole, the actin filaments increase both their size and number (19).

As shown in Fig. S4, in buffer, the fluctuations induced by the cells on the cantilever sensor evidence a constant basal activity intercalated by large (>10 nm) and smaller (>2 nm) movement spikes.

The introduction of nocodazole (0.2 μg/mL) rapidly depolymerizes the tubulin network and has a large effect on the morphology of the cells on the cantilever. On the other hand, probably because the tubulin network is located deeper inside the cell cytoskeleton, its contribution to the fluctuations of the sensor is not as evident as in the actin case. However, even in this challenging scenario, the very high sensitivity of the nanomotion detector allows discriminating some small variations. Indeed, the fluctuations graph shows that the component that disappears upon injection of nocodazole is the small, >2-nm spikes whereas the basal fluctuations and the large spikes are still present. This result suggests that these smaller fluctuations could be the representation of the movements of the tubulin network.

1. Gamborg OL, Miller RA, Ojima K (1968) Nutrient requirements of suspension cultures of soybean root cells. *Exp Cell Res* 50(1):151–158.
2. Kasas S, et al. (2013) A universal fluid cell for the imaging of biological specimens in the atomic force microscope. *Microsc Res Tech* 76(4):357–363.
3. Thomson NH, Kasas S, Smith B, Hansma HG, Hansma PK (1996) Reversible binding of DNA to mica for AFM imaging. *Langmuir* 12(24):5905–5908.
4. Louise Meyer R, et al. (2010) Immobilisation of living bacteria for AFM imaging under physiological conditions. *Ultramicroscopy* 110(11):1349–1357.
5. Howarter JA, Youngblood JP (2006) Optimization of silica silanization by 3-aminopropyltriethoxysilane. *Langmuir* 22(26):11142–11147.
6. Benoit M, Gabriel D, Gerisch G, Gaub HE (2000) Discrete interactions in cell adhesion measured by single-molecule force spectroscopy. *Nat Cell Biol* 2(6):313–317.
7. Florin EL, Moy VT, Gaub HE (1994) Adhesion forces between individual ligand-receptor pairs. *Science* 264(5157):415–417.
8. Hutter JL, Bechhoefer J (1993) Calibration of atomic-force microscope tips. *Rev Sci Instrum* 64(7):1868–1873.
9. Hammonds TR, Maxwell A (1997) The DNA dependence of the ATPase activity of human DNA topoisomerase IIalpha. *J Biol Chem* 272(51):32696–32703.
10. Bertin P, et al. (1994) The H-NS protein is involved in the biogenesis of flagella in Escherichia coli. *J Bacteriol* 176(17):5537–5540.
11. Wadhams GH, Armitage JP (2004) Making sense of it all: Bacterial chemotaxis. *Nat Rev Mol Cell Biol* 5(12):1024–1037.
12. Lai HC, et al. (1997) Effect of glucose concentration on swimming motility in enterobacteria. *Biochem Biophys Res Commun* 231(3):692–695.
13. Shi W, Li C, Louise CJ, Adler J (1993) Mechanism of adverse conditions causing lack of flagella in Escherichia coli. *J Bacteriol* 175(8):2236–2240.
14. Li C, Louise CJ, Shi W, Adler J (1993) Adverse conditions which cause lack of flagella in Escherichia coli. *J Bacteriol* 175(8):2229–2235.
15. Kearns DB (2010) A field guide to bacterial swarming motility. *Nat Rev Microbiol* 8(9):634–644.
16. Ailenberg M, Silverman M (2003) Cytochalasin D disruption of actin filaments in 3T3 cells produces an anti-apoptotic response by activating gelatinase A extracellularly and initiating intracellular survival signals. *Biochim Biophys Acta* 1593(2–3):249–258.
17. Jones JL, Davis WL, Jones RG, Miller GW, Matthews JL (1977) The effect of cytochalasin B on the endosteal lining cells of mammalian bone: A scanning electron microscopic study. *Calcif Tissue Res* 24(1):1–10.
18. Samson F, Donoso JA, Heller-Bettinger I, Watson D, Himes RH (1979) Nocodazole action on tubulin assembly, axonal ultrastructure and fast axoplasmic transport. *J Pharmacol Exp Ther* 208(3):411–417.
19. Smurova KM, Birukova AA, Verin AD, Alieva IB (2008) Dose-dependent effect of nocodazole on endothelial cell cytoskeleton. *Biochem. Moscow Suppl. Ser. A* 2(2):119–127.

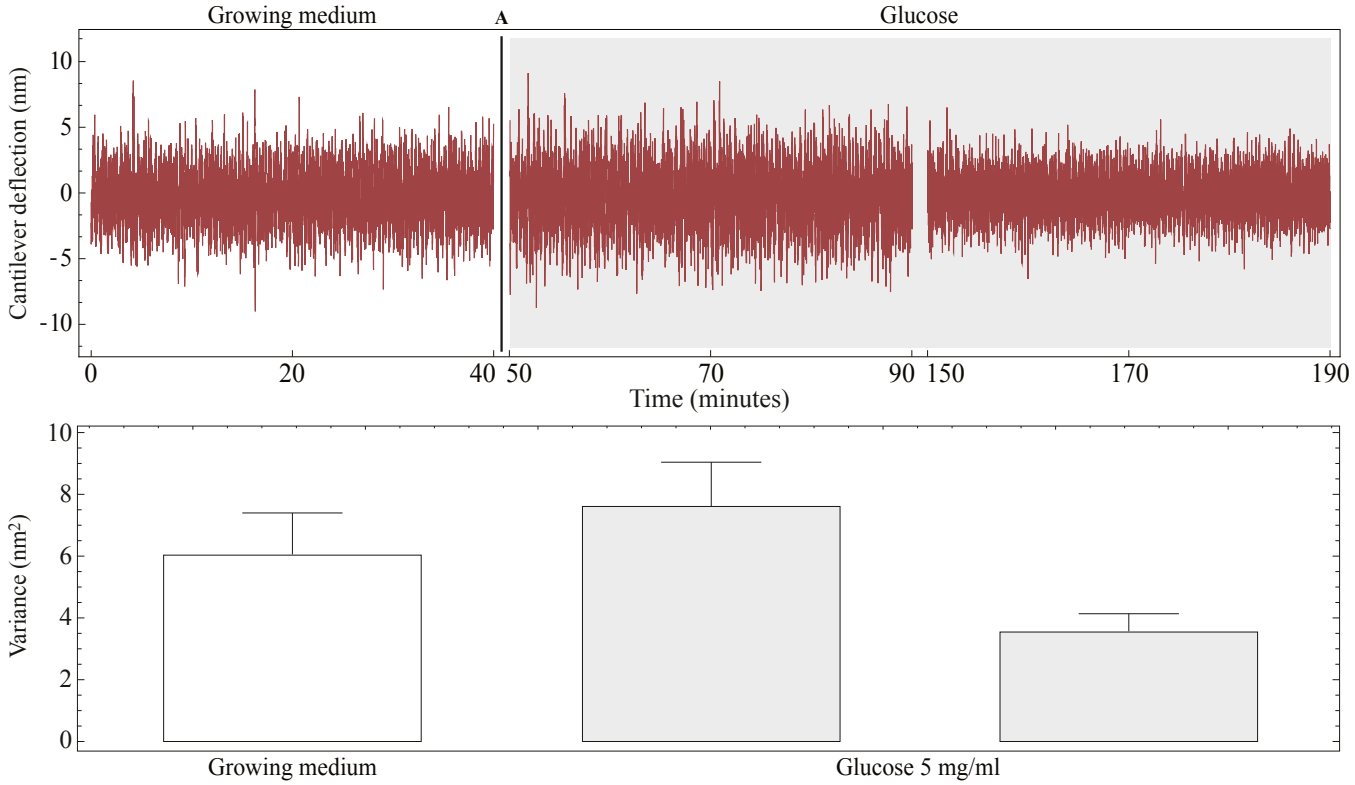

Fig. S1. Experiment to determine the effect of the movements of the flagella in *E. coli*. Three typical 40-min segments of the sensor's fluctuations are shown: the bacteria in conventional growing medium induced a large fluctuation of the sensor. Just after the injection of 5 mg/mL glucose, the movement increases. Such increase is followed by a decrease, probably due to the reduction of the movements of the bacterial flagella.

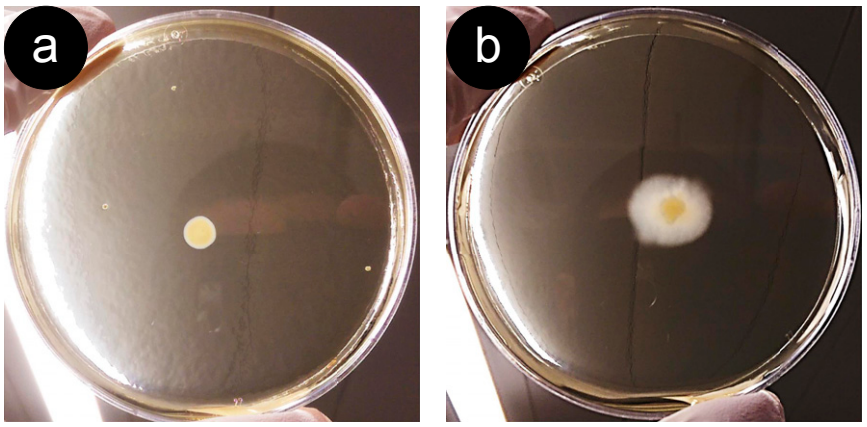

Fig. S2. Swarming tests. Small aliquots of bacteria grown in LB with (*A*) and without (*B*) glucose were inserted into fluid agar and incubated for 40 h. The bacteria grown in glucose is not swarming, as demonstrated by the small and well-defined colony. The bacteria grown in LB have working and active flagella, as shown by the larger and less-defined colony.

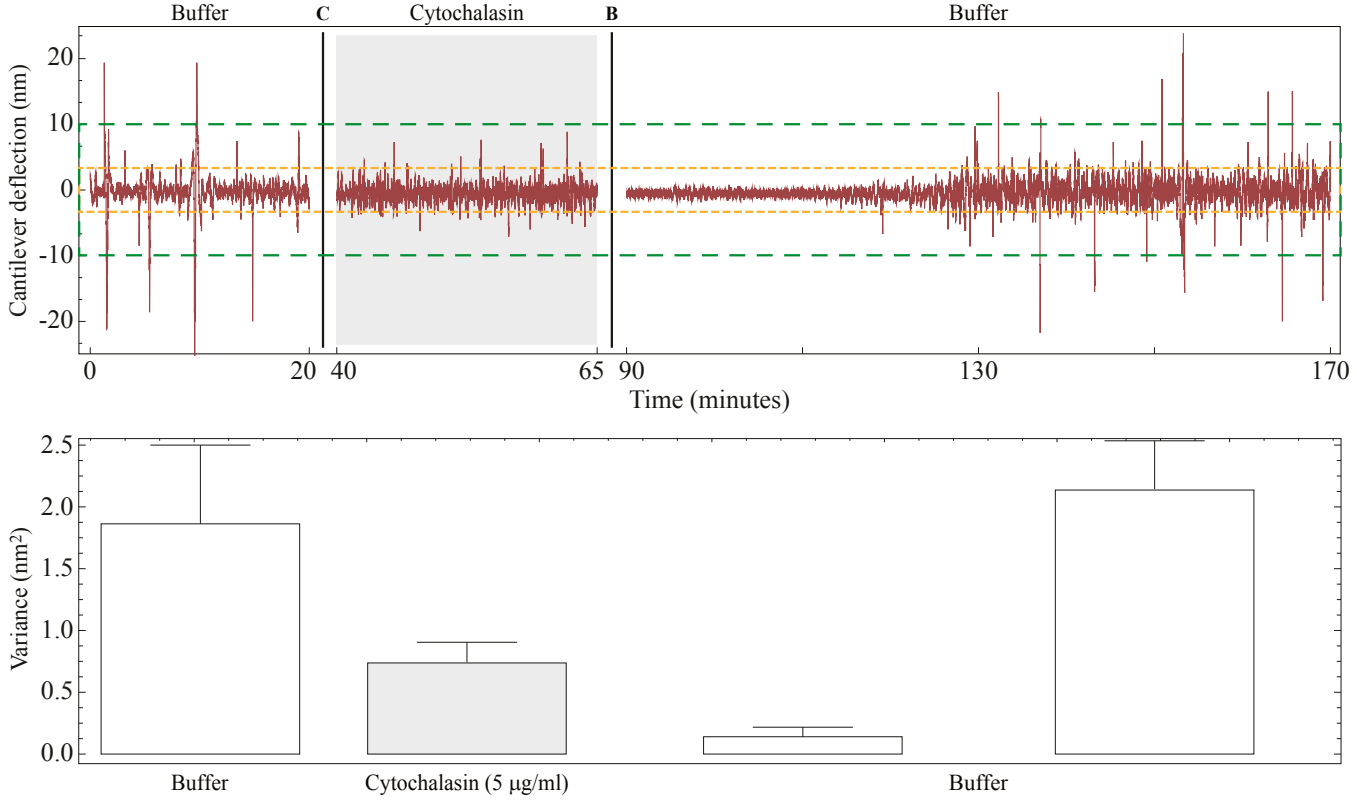

Fig. S3. Experiment to determine the effect of the movements of the actin network in osteoblasts. Three typical segments of the sensor's fluctuations are shown: the osteoblasts in growing buffer induce fluctuations of the sensor that can be divided in large spikes (outside the green area), smaller spikes (between the green and the orange areas), and a basal fluctuation. Just after the injection of 5 μg/mL cytochalasin, only one of these components is affected: the large spikes. The basal fluctuations and the smaller spikes are still present. This change in the fluctuation pattern is reversible: When the chemical agent is removed, the cells undergo a reorganization period, followed by a return to the normal fluctuation, with all three components.

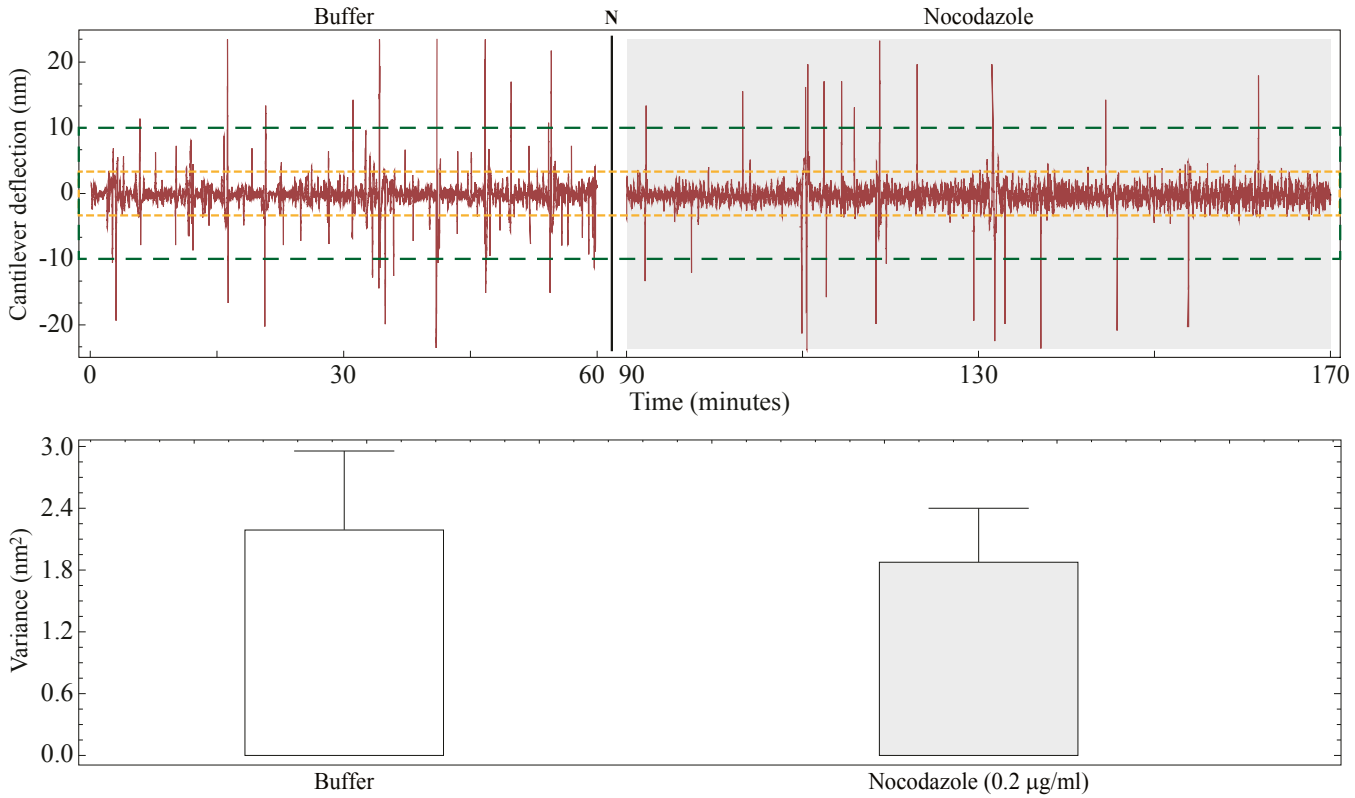

Fig. S4. Experiment to determine the effect of the movements of the tubulin network in osteoblasts. Two typical segments of the sensor's fluctuations are shown. The osteoblasts in growing buffer evidence the three fluctuation components: large spikes, small spikes, and basal fluctuations. Just after the injection of 0.2 μg/mL nocodazole, only one of these components seems to be affected: the small spikes. The basal fluctuations and the large spikes are still present. Remarkably, the overall variance levels exhibit only small changes after the depolymerization of the tubulin network.

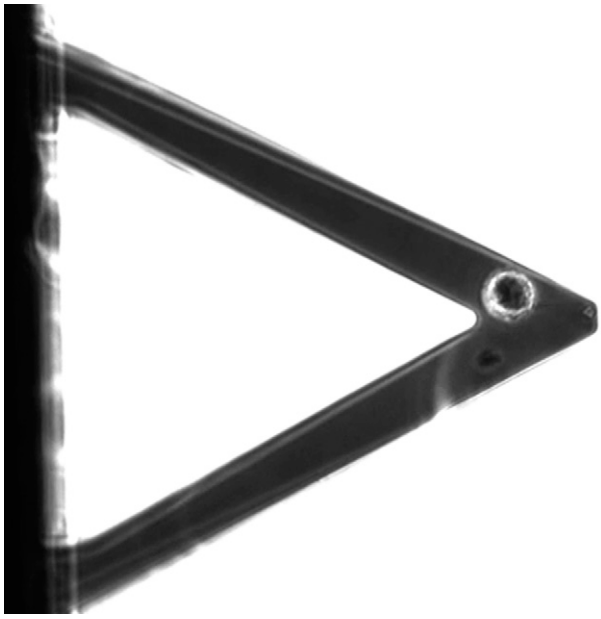

Movie S1. Time-lapse movie of the movements of an osteoblast cell on the surface of a cantilever. The cell can be seen spreading over the apical area of the cantilever. The images were collected every 20 s, and the movie is encoded at 20 fps.

Movie S1

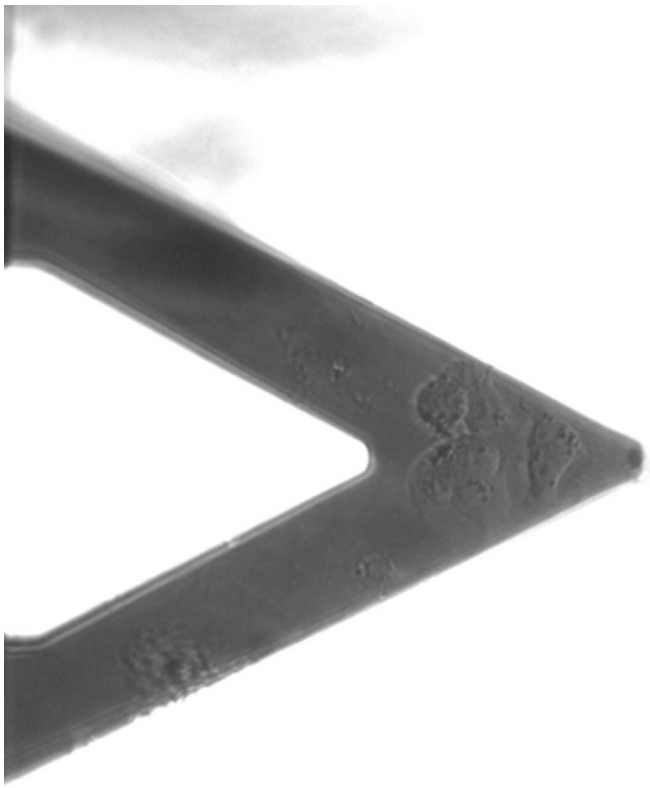

Movie S2. Time-lapse movie of the movements of several neuroblast cells on the surface of a cantilever. The cells are well attached to the surface, and some movement can be seen. The images were collected every 20 s, and the movie is encoded at 20 fps.

Movie S2

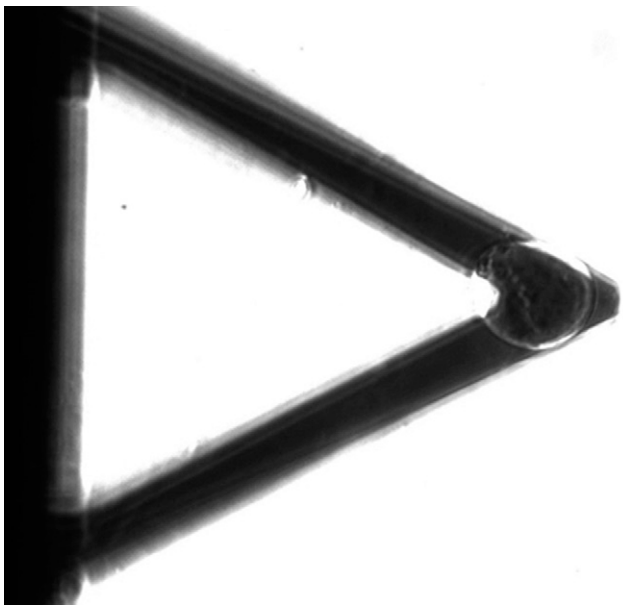

Movie S3. Time-lapse movie of an *A. thaliana* cell attached to the surface of a cantilever. The cell does not seem to be moving, but several compartments and vacuoles are moving inside the cell cytoplasm. The images were collected every 20 s, and the movie is encoded at 20 fps.

Movie S3

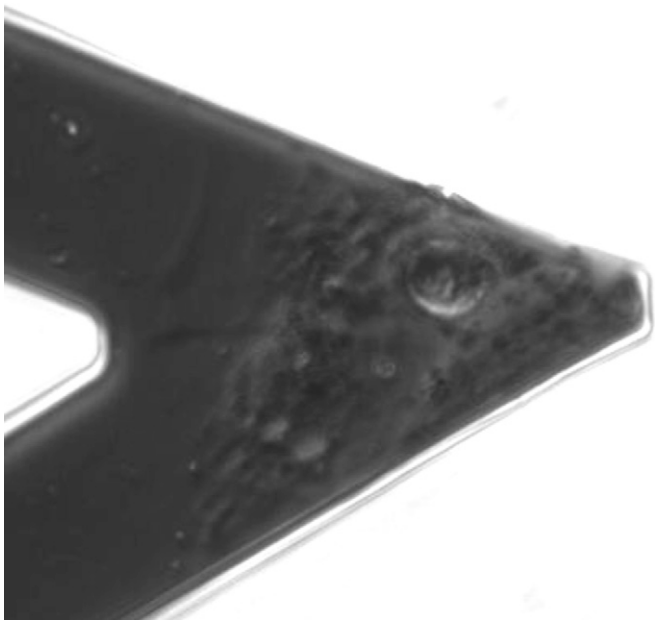

Movie S4. Time-lapse movie of the movements of an osteoblast cell on the surface of a cantilever exposed to cytochalasin. In buffer, the cells have spread over the apical area of the cantilever (0–4 s). Upon the injection of the drug, the cells lose their overall morphology, shrink, and their movements are reduced (4–24 s). By removing the drug, the cells are able to reconstruct their actin network and return to a normal activity (24–54 s). In this case, the actin rearrangements reappear (38–54 s). The images were collected every 20 s, and the movie is encoded at 20 fps.

Movie S4

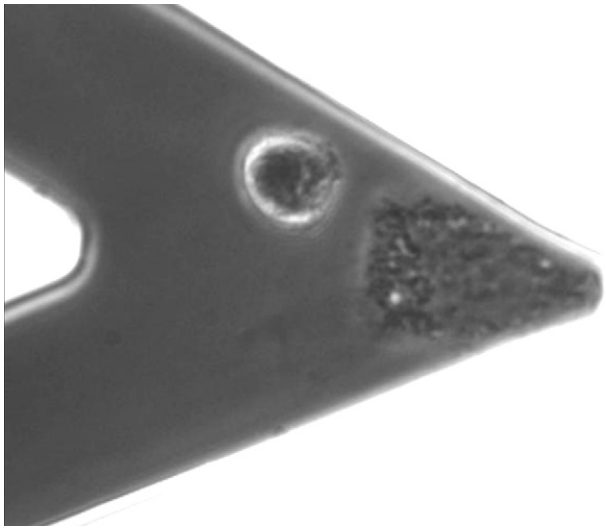

Movie S5. Time-lapse movie of the movements of an osteoblast cell on the surface of a cantilever exposed to nocodazole. At first, the cells are spread over the apical area of the cantilever. After introducing the drug, the cells partially lose their overall morphology but maintain some structural integrity. Even in the presence of the drug, we can clearly see movements in the cellular appendages, which are compatible with rearrangements of the actin network (3–15 s). The images were collected every 20 s, and the movie is encoded at 20 fps.

Movie S5